



Discovery of 5-pyrrolopyridinyl-2-thiophenecarboxamides as potent AKT kinase inhibitors

Mark A. Seefeld^{a,*}, Meagan B. Rouse^a, Kenneth C. McNulty^a, Lihui Sun^a, Jizhou Wang^a, Dennis S. Yamashita^a, Juan I. Luengo^a, ShuYun Zhang^b, Elisabeth A. Minthorn^c, Nestor O. Concha^d, Dirk A. Heering^a

^aOncology Chemistry, GlaxoSmithKline, Collegeville, PA 19426, USA

^bOncology Biology, GlaxoSmithKline, Collegeville, PA 19426, USA

^cDrug Metabolism and Pharmacokinetics, GlaxoSmithKline, Collegeville, PA 19426, USA

^dComputational, Analytical and Structural Sciences, GlaxoSmithKline, Collegeville, PA 19426, USA

ARTICLE INFO

Article history:

Received 28 January 2009

Revised 23 February 2009

Accepted 24 February 2009

Available online 27 February 2009

Keywords:

AKT

Kinase

ABSTRACT

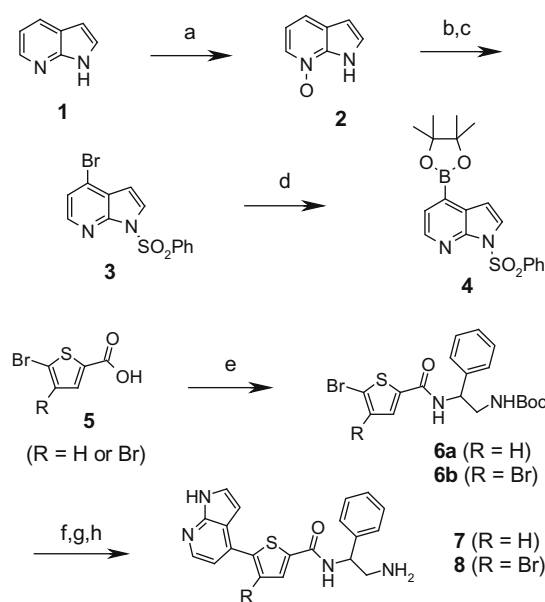
A pyrrolopyridinyl thiophene carboxamide **7** was discovered as a tractable starting point for a lead optimization effort in an AKT kinase inhibition program. SAR studies aided by a co-crystal structure of **7** in AKT2 led to the identification of AKT inhibitors with subnanomolar potency. Representative compounds showed antiproliferative activity as well as inhibition of phosphorylation of the downstream target GSK3 β .

© 2009 Elsevier Ltd. All rights reserved.

AKT, also known as protein kinase B (PKB), is a serine/threonine kinase from the AGC family of kinases that exists in three homologous human isoforms (AKT1, AKT2, AKT3). AKT plays a critical role in signal transduction and apoptotic pathways effecting cell survival and proliferation.¹ Over-expression of AKT has an anti-apoptotic effect in many cell types.² In addition, PTEN, a critical negative regulator of AKT, is mutated or lost in many cancers including breast, ovarian, prostate carcinomas and glioblastomas.³ Therefore, inhibition of the AKT signalling pathway offers a viable strategy for the treatment of cancers.⁴

In a previous communication,⁵ we described the discovery and development of an aminofurazan series of AKT inhibitors. Although potent AKT inhibition was achieved, this series suffered from poor oral exposure in preclinical species. Therefore, alternative chemotypes were examined to try to find AKT inhibitors suitable for oral delivery. Compounds based on pyrrolopyridinyl thiophene carboxamides (chemotype **7**, Scheme 1) were identified as low nanomolar ATP-competitive inhibitors of AKT1 through a screening of the GSK kinase inhibitor collection. Pan-AKT activity is likely given the sequence similarity of AKT2 (90%) and AKT3 (88%) to AKT1 in the kinase domain.^{6,7}

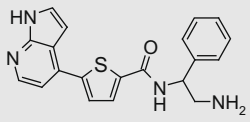
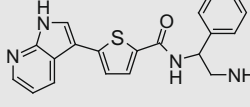
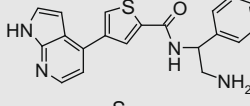
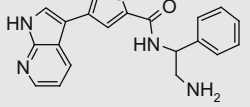
Synthesis of pyrrolopyridinyl thiophene amides began with the construction of boronate **4**.⁸ 7-Azaindole (**1**) was oxidized to the



Scheme 1. Reagents and conditions: (a) MCPBA, CHCl_3 , 59%; (b) $(\text{CH}_3\text{SO}_2)_2\text{O}$, $(\text{CH}_3)_4\text{NBr}$, DMF, 40%; (c) PhSO_2Cl , Et_3N , DCM, 95%; (d) $\text{Pd}(\text{dppf})_2\text{Cl}_2$, bis(pinacolato)diboron, KOAc, DMF, 81%; (e) PyBrop, Et_3N , 1,1-dimethylethyl(2-amino-2-phenylethyl) carbamate, DCM, rt, 80%; (f) $\text{Pd}(\text{PPh}_3)_4$, K_2CO_3 , dioxane/ H_2O , 70 °C, 65–79%; (g) NaOH, MeOH/THF/ H_2O , rt; (h) HCl, dioxane, rt, quant.

* Corresponding author. Tel.: +1 610 917 7936; fax: +1 610 917 4206.
E-mail address: mark.a.seefeld@gsk.com (M.A. Seefeld).

Table 1Effect of pyrrolopyridine and thiophene regiochemistry on AKT1 enzyme and mechanistic activities for compounds **7** and **9–11**

Compound	Structure	AKT1 IC ₅₀ ^a (nM)	pGSK3β IC ₅₀ ^b (nM)
7		6	190
9		16	240
10		40	1000
11		25	1100

^a Values are measured against AKT1 at or below K_m for ATP; $n \geq 2$.^b Inhibition of phosphorylation of GSK3β in BT474 cells.

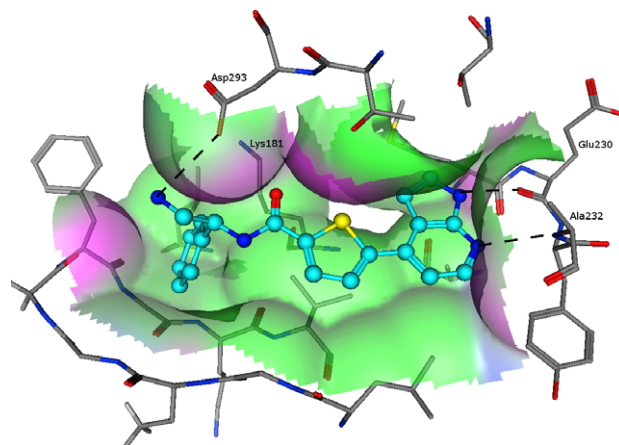
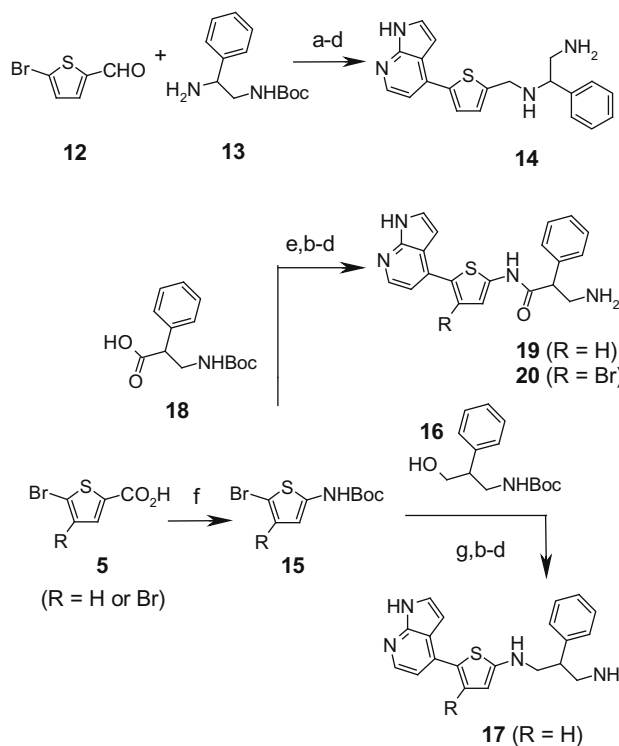
N-oxide **2**, which was treated with methanesulfonic anhydride and tetramethyl ammonium bromide to afford 4-bromo-pyrrolopyridine.

Reaction with phenylsulfonyl chloride provided the 4-bromo pyrrolopyridine **3**. Formation of the boronic ester⁹ using bis (pinacolato)diboron gave **4**. The coupling partner **6** was prepared by the PyBrop-mediated reaction of commercially available Boc-1-amino-2-phenyl ethylamine with bromothiophene carboxylate **5**. Suzuki coupling of **4** and **6**, followed by sequential deprotection under basic and then acidic conditions, yielded amide **7**. Compound **8** was made by coupling boronate **4** with the dibromothiophene intermediate **6b**. Regiochemical assignment of **8** was confirmed by NMR studies. Compounds **9–11** were similarly prepared using bromothiophene 2-carboxylic acids and 1-(phenylsulfonyl)-3-(4,4,5,5-tetramethyl-1,3,2-dioxaborolan-2-yl)-1*H*-pyrrolo[2,3-*b*]pyridine¹⁰ as appropriate.

Initially, we were interested to determine if **7** represented the optimal orientation of the pyrrolopyridine, therefore we conducted a regioisomeric assessment of the core thiophene and its activity relationship with the pyrrolopyridine moiety (Table 1). The 2,5-disubstituted thiophene **7** gave slightly improved AKT enzyme inhibition relative to regioisomers **9–11**. Compounds **7** and **9** demonstrated a more pronounced effect on the inhibition of phosphorylation levels of downstream target GSK3β.¹¹ The attachment of the thiophene to the pyrrolopyridine at either the 3-position or the 4-position had little effect on overall activity with a minor preference for the 4-position regiochemistry as measured in the cell-based mechanistic assay (pGSK3β). The modest effect of these regioisomers on AKT activity suggests that the thiophene acts primarily as a lipophilic link between the pyrrolopyridine hinge and the amide functionality.

We next turned our attention to understanding the interactions of the linking amide of **7** with AKT. An X-ray co-crystal structure of **7** (AKT2 IC₅₀ = 50 nM) was determined to 2.3 Å resolution in AKT2 (Fig. 1).¹² Based on this structure, it is evident that the amide carbonyl of **7** was 4.4 Å away from the terminal nitrogen of Lys181. We proposed that the amide carbonyl interacts with this lysine residue of AKT2, possibly via a molecule of water. Although we were unable to detect this interaction in our co-crystal structure, others have observed it in similar systems.¹³

We then investigated various replacements of the amide linker in **7** with methylamine and reverse amide linkers. Compound **14**

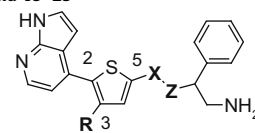
**Figure 1.** X-ray structure of **7** co-crystallized in AKT2 (146–481).

Scheme 2. Reagents and conditions: (a) NaBH₄, EtOH/DCM, rt, 75% (b) Pd(PPh₃)₄, K₂CO₃, **4**, dioxane/H₂O, 70 °C, 65–79%; (c) NaOH, MeOH/THF/H₂O, rt; 85–95% (d) HCl, dioxane, rt, quant (e) PyBrop, Et₃N, DCM, rt, 80%; (f) DPPA, *t*-BuOH, dioxane, 70 °C, 60%; (g) DIAD, **16**, PPh₃, THF, rt, 75%.

was constructed by combining aldehyde **12** and amine **13** under reductive amination conditions and further elaborating as described in Scheme 2. Amino thiophene **15** was obtained by subjecting **5** to Curtius reaction conditions.¹⁴ The Boc-protected amine **15** underwent a Mitsunobu reaction with alcohol **16** to ultimately provide amine **17**. Alternatively, thiophene **15** was deprotected and coupled to carboxylic acid **18** using PyBrop. A subsequent Suzuki reaction and deprotection steps yielded reverse amides **19** and/or **20**. Substituents at position-3 (R, Table 2) were appended using a Suzuki reaction with a Boc-protected version of bromide **8** and the appropriate boronate.

The amide functionality of **7** clearly imparts a beneficial effect as the levels of AKT1 activity and mechanistic activity (inhibition of GSK3β phosphorylation) were significantly reduced in its absence (**14** and **17**, Table 2). The reverse amide compound **19**

Table 2
Thiophene substituent and amide regiochemistry effects on AKT1 and GSK3 β for compounds **7**, **8**, **14**, **17** and **19–25**



Compound	R	X	Z	AKT1 IC ₅₀ ^a (nM)	pGSK3 β IC ₅₀ ^b (nM)
7	H	C=O	NH	6	190
14	H	CH ₂	NH	100	>10,000
17	H	NH	CH ₂	250	>10,000
19	H	NH	C=O	3	560
20	Br	NH	C=O	25	4700
8	Br	C=O	NH	8	500
21	CH ₃	C=O	NH	8	120
22	c-Pr	C=O	NH	6	800
23	Ph	C=O	NH	50	10,000
24		C=O	NH	63	6000
25		C=O	NH	63	2500

^a Values are measured against AKT1 at or below K_m for ATP; $n \geq 2$.

^b Inhibition of phosphorylation of GSK3 β in BT474 cells.

produced comparable levels of enzyme inhibition, but with reduced inhibition of AKT mediated GSK3 β phosphorylation.

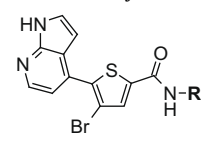
The bromine substituent on reverse amide **20** was less tolerated. The potential for the thiophene ring to rotate 180° from the orientation shown in Figure 1 cannot be discounted and may contribute to the difference in activity of **20** relative to **8**. Small lipophilic functionality (Br, Me and c-Pr; **8**, **21**, **22**, respectively) was tolerated at position R on the thiophene of amide **7**. Larger aromatic substituents (**23–25**) reduced AKT1 activity. This was in keeping with the compact lipophilic environment of the ATP binding pocket.

We then systematically investigated the nature of the amide substituent (Table 3). The bromo group on the thiophene ring was left intact as a potential source for further structural elaboration as we evaluated amide group modifications. Removing (**26**) or shifting the position of the phenyl substituent (**27**) reduced AKT activity and was deleterious to inhibition of GSK3 β phosphorylation. Lengthening the alkyl amine (**30**, **31**) also proved to be of no benefit. Secondary amines (**28**, **33**) were tolerated, however more sterically demanding amines (**34**, **35**) caused a reduction in activity, presumably by interfering with the ability of the pendant amine to bind to Asp293. Tertiary amine **29** showed no detectable activity in the pGSK3 β assay. Primary amine **32** exhibited the best combination of enzyme and mechanism-based activity, and was selected for further investigation (Table 4).

The required diamines were prepared from commercially available amino acids (Scheme 3). Reduction of the carboxylic acid of **36** with BH₃·THF followed by a Mitsunobu reaction between the resultant alcohol and phthalimide provided a differentially protected diamine which when treated with HCl in dioxane gave **37**. Cyclohexyl (**40**) and pyridyl (**41**) analogs (Table 4) were similarly prepared.

The (*R*)-enantiomer **38** was found to be several hundred times less active in the AKT kinase assays than the corresponding (*S*)-enantiomer **39**. The most potent combination of enzyme and cellular activity was provided by small lipophilic functionality. Electron withdrawing groups on the phenyl ring (**43–48**), in general, showed an improvement in the inhibition of proliferation in cell lines that have been previously demonstrated to be sensitive to AKT (BT474, LNCaP)^{15,16} relative to cell lines that are nontumor derived (HFF). However, considerable inhibition of HFF cells nonetheless remains

Table 3
Effect of amines **8** and **26–35** on AKT activity



Compound	R	AKT1 IC ₅₀ ^a (nM)	pGSK3 β IC ₅₀ ^b (nM)
26		158	>10,000
27		40	>10,000
8		8	500
28		3	780
29		20	>10,000
30		8	1500
31		20	4800
32		1	80
33		2	260
34		4	1100
35		10	2100

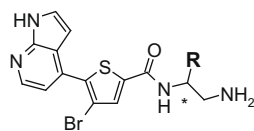
^a Values are measured against AKT1 at or below K_m for ATP; $n \geq 2$.

^b Inhibition of phosphorylation of GSK3 β in BT474 cells.

and may indicate activities unrelated to AKT inhibition. Subnanomolar AKT1 inhibition was required to demonstrate good anti-proliferative activity from compounds of this series. For compounds that approached the tight binding limit of the IC₅₀ assay, we used an alternative assay format (K_i^+)¹⁷ which allowed for measurement of subnanomolar potencies. This assay was run in parallel with our standard high throughput AKT enzyme assay.¹¹

In order to characterize the pharmacokinetic performance of representative 5-pyrrolopyridinyl-thiophene amides, compounds **8** and **32** were evaluated in iv/po crossover studies in rat (Table 5). These two compounds differ structurally by only a methylene group, yet this minor change appears to be responsible for a several fold increase in AKT activity. The PK profile for compound **8** shows moderate clearance and oral exposure with a consequence of modest oral bioavailability. The benzyl compound (**32**) shows generally poorer PK. The oral bioavailability of benzyl compound **32**, although similar to phenyl compound **8** in average value, ranged from 6% to 70%. This variable oral bioavailability is characteristic of all the benzyl analogs tested in Table 4. While the PK profile of the benzyl compounds were less than optimal they were sufficient to conduct PD studies. Compound **44** exhibited potent overall in vitro activity and was therefore chosen to be tested for a pharmacodynamic (PD) response in BT474 tumor bearing xenograft mice. The effect of compound **44** on the inhibition of GSK3 β phosphorylation was measured at three doses (6.25, 12.5 and 25 mg/kg) following a single ip injection. Tumors were harvested 4 h post dose. Figure 2 illustrates the dose-dependent reduction in pGSK3 β levels produced by compound **44** in mice relative to vehicle.

Table 4
AKT activity and cell potency derived from benzyl group manipulations



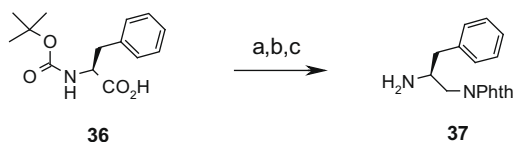
Compound	Chirality	R	Kinase Activity ^a (nM)			Cellular Activity ^c IC ₅₀ (nM)			
			AKT1 IC ₅₀ [<i>K</i> _i ']	AKT2 IC ₅₀ [<i>K</i> _i ']	AKT3 IC ₅₀	pGSK3β ^b	BT474	LNCaP	HFF
8	(±)	Phenyl	8 [20]	125 [125]	20	500	4000	750	1200
32	(±)	Benzyl	1 [0.04]	13 [8]	3	80	200	45	410
38	R	Benzyl	32 [20]	500 [800]	40	6000	4500	2700	1900
39	S	Benzyl	1 [0.06]	10 [3]	2	100	230	21	90
40	S	Cyclohexyl-CH ₂ -	1 [0.79]	25 [6]	3	1900	2600	440	NT
41	S	4-Pyridyl-CH ₂ -	[2]	[40]	NT	1900	2300	750	3600
42	S	4-Methoxybenzyl	3 [5]	63 [40]	2	1000	1900	720	890
43	S	2-Fluorobenzyl	1	8	2	220	120	39	260
44	S	3-Fluorobenzyl	1 [0.03]	9 [0.63]	2	90	240	18	260
45	S	4-Fluorobenzyl	1 [0.06]	6 [2]	2	180	500	66	490
46	S	2-Trifluoromethylbenzyl	3 [0.05]	25 [4]	2	50	60	24	730
47	S	3-Trifluoromethylbenzyl	1 [0.10]	10 [4]	1	170	60	78	530
48	S	4-Trifluoromethylbenzyl	2 [2]	79 [16]	3	2000	1200	440	1300

NT = not tested.

^a Values are an average of at least 2 measurements.

^b Inhibition of phosphorylation of GSK3β in BT474 cells.

^c Inhibition of cell proliferation.



Scheme 3. Reagents and conditions: (a) BH₃·THF, 0 °C, 89%; (b) DIAD, phthalimide, PPh₃, THF, rt, 95%; (c) HCl, dioxane, rt, quant.

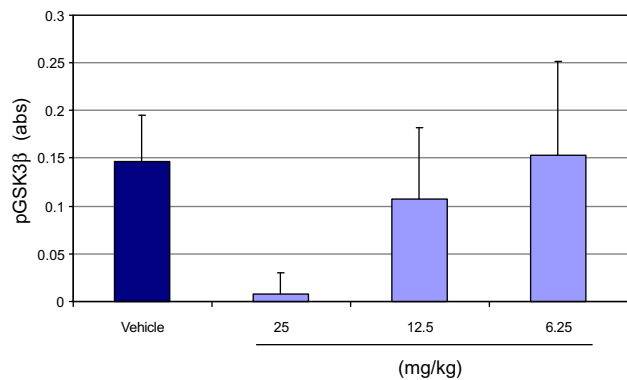
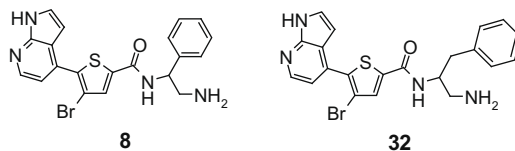


Figure 2. Effect of **44** on GSK3β phosphorylation levels in BT474 xenograft mice after 4 h. Vehicle: 5% dextrose, pH 4.0.

Table 5
iv/po crossover studies for compounds **8** and **32** in conscious male rats (*n* = 3)



Compound	iv/po ^{a,b} (mg/kg)	C _{max} (ng/mL)	Cl (mL/min/kg)	T _{1/2} (h)	AUC _(0-t) (ng h/mL)	%F
8	iv (2)	1800	16.7	3.6	3248	32
	po (10)	550		4.1	3397	
32	iv (2)	712	49	3.8	893	38
	po (10)	248		ND	664	

^a iv: fed, solution in 1% DMSO, 20% encapsin in saline. po: fasted, solution in 1% DMSO, 20% PEG400 in water; pH 3.0–3.5.

^b Blood samples were collected over 24 h.

Table 6
Activity of **44** on various kinases

Kinase family	Kinases ^a	44 , IC ₅₀ (nM)
AGC	AKT1 ^b	0.03
	AKT2 ^b	8
	AKT3	2
	PKCα	40
	ROCK1	2
CMGC	GSK3β	20,000
	P38α	25,000
CAMK	MAPKAPK2	2500
	PIM-1	794
TK	EGFR	10,000
	SYK	25,000

^a All kinase IC₅₀s were assayed at or below *K*_m for ATP.

^b Values determined as *K*_i'.

The selectivity profile of compound **44** was evaluated against a panel of >50 different kinases, of which representative examples are shown (Table 6). The results depict a pattern of moderate to poor selectivity against the AGC family of kinases where a high homology with the AKT active site exists. A much better selectivity profile was achieved against protein kinases from other kinase families.

In summary, we have demonstrated that pyrrolopyridinyl thiophene amides are potent pan-AKT inhibitors. Compounds from

this series showed cellular activity that correlated well with inhibition of phosphorylation of the AKT downstream target GSK3 β . Dose-dependent inhibition of GSK3 β phosphorylation was demonstrated in an in vivo pharmacodynamic model for a representative compound. The oral bioavailability of compounds across this series in preclinical species demonstrated a significant improvement from our earlier series of AKT inhibitors.⁵ The co-crystal structure of **7** will be used to guide further structural refinements with a goal of improving kinase selectivity and PK parameters.

Acknowledgments

The authors would like to thank Melissa Dumble, Kim Robell, Dana Levy, Michael Schaber, Anthony Choudhry, Zhihong Lai, Rakesh Kumar and Jason Kahana for helpful discussions. We would also like to thank Kristin Koretke for molecular modelling assistance.

Supplementary data

Supplementary data associated with this article can be found, in the online version, at doi:10.1016/j.bmcl.2009.02.094.

References and notes

- For reviews on AKT see: (a) Bellacosa, A.; Kumar, C.; Di Cristofano, A.; Testa, J. R. *Adv. Cancer Res.* **2005**, *94*, 29; (b) Li, Q.; Zhu, G.-D. *Curr. Top. Med. Chem.* **2002**, *2*, 939.
- Jetzt, A.; Howe, J. A.; Horn, M. T.; Maxwell, E.; Yin, Z.; Johnson, D.; Kumar, C. C. *Cancer Res.* **2003**, *63*, 6697.
- (a) Sansal, I.; Sellers, W. R. J. *Clin. Oncol.* **2004**, *22*, 2954; (b) Hsu, J. H.; Shi, Y.; Hu, L.; Fisher, M.; Franke, T. F.; Lichtenstein, A. *Oncogene* **2002**, *21*, 1391.
- (a) Lindsley, C. W.; Barnett, S. F.; Yaroschak, M.; Bilodeau, M. T.; Layton, M. E. *Curr. Top. Med. Chem.* **2007**, *7*, 1349; (b) Heerding, D. A.; Safonov, I. G.; Verma, S. K. *Ann. Rep. Med. Chem.* **2007**, *42*, 365.
- Heerding, D. A.; Rhodes, N.; Leber, J. D.; Clark, T. J.; Keenan, R. M.; LaFrance, L. V.; Li, M.; Safonov, I. G.; Takata, D. T.; Venslavsky, J. W.; Yamashita, D. S.; Choudhry, A. E.; Copeland, R. A.; Lai, Z.; Schaber, M. D.; Tummino, P. J.; Strum, S. L.; Wood, E. R.; Duckett, D. R.; Eberwein, D.; Knick, V. B.; Lansing, T. J.; McConnell, R. T.; Zhang, S.-Y.; Minthorn, E. A.; Concha, N. O.; Warren, G. L.; Kumar, R. J. *Med. Chem.* **2008**, *51*, 5663.
- Kumar, C. C.; Madison, V. *Oncogen* **2005**, *24*, 7493.
- Allosteric inhibitors have recently been described that show AKT isoform selectivity. See reference: *Bioorg. Med. Chem. Lett.* **2009**, *19*, 834.
- Seefeld, M. A.; Hamajima, T.; Jung, D. K.; Nakamura, H.; Reid, P. R.; Reno, M. J.; Rouse, M. B.; Heerding, D. A.; Tang, J.; Wang, J.; PCT Patent App. WO 2007076423 A2, 2007.
- Ishiyama, T.; Murata, M.; Miyaura, N. *J. Org. Chem.* **1995**, *60*, 7508.
- Huang, S.; Li, R.; Connolly, P. J.; Emanuel, S.; Middleton, S. A. *Bioorg. Med. Chem. Lett.* **2006**, *16*, 4818.
- For details of in vitro kinase inhibition assays and assays used to measure inhibition of GSK3 β phosphorylation see: Rhodes, N.; Heerding, D. A.; Duckett, D. R.; Eberwein, D. J.; Knick, V. B.; Lansing, T. J.; McConnell, R. T.; Gilmer, T. M.; Zhang, S. Y.; Robell, K.; Kahana, J. A.; Geske, R. S.; Kleymenova, E. V.; Choudhry, A. E.; Lai, Z. V.; Leber, J. D.; Minthorn, E. A.; Strum, S. L.; Wood, E. R.; Huang, P. S.; Copeland, R. A.; Kumar, R. *Cancer Res.* **2008**, *68*, 2366.
- Crystallographic data for compound **7** has been deposited in the PDB with deposition code 3E87. The level of resolution does not permit the assignment of specific stereochemistry.
- Lin, X.; Murray, J. M.; Rico, A. C.; Wang, M. X.; Chu, D. T.; Zhou, Y.; Del Rosario, M.; Kaufman, S.; Ma, S.; Fang, E.; Crawford, K.; Jefferson, A. B. *Bioorg. Med. Chem. Lett.* **2006**, *16*, 4163.
- Thornton, T. J.; Jarman, M. *Synthesis* **1990**, *4*, 295.
- Rusnak, D. W.; Lackey, K.; Affleck, K.; Wood, E. R.; Alligood, K. J.; Rhodes, N.; Keith, B. R.; Murray, D. M.; Knight, W. B.; Mullin, R. J.; Gilmer, T. M. *Mol. Cancer Ther.* **2001**, *1*, 85.
- Nakatani, K.; Thompson, D. A.; Barthel, A.; Sakaue, H.; Liu, W.; Weigel, R. J.; Roth, R. A. *J. Biol. Chem.* **1999**, *274*, 21528.
- K_i^* values were determined against human or mouse AKT1 and AKT2 as follows: Either AKT1 (30 μ L, final concentration 0.33 nM) or AKT2 (30 μ L, final concentration 1 nM) in buffer A were added to 2 μ L inhibitor at various concentrations. AKT and inhibitor were incubated for 60 min at room temperature. The reaction was initiated by adding 8 μ L of substrate mix in buffer A containing GSK3 α peptide (final concentration 10 μ M), ATP (final concentration 50 μ M), and γ -³³P-ATP (final concentration 0.03 mCi/mL). After 120 min, the reaction was stopped with 40 μ L of 1% H₃PO₄. The stopped reaction was transferred to phosphocellulose filter plates and washed 5 times with 100 μ L of 0.5% H₃PO₄. Microscint20 cocktail was added to the dried filter plates and read using a Perkin Elmer Microbeta liquid scintillation counter. K_i^* values were calculated using the following equation:

$$IC_{50} = [E]/2 + K_i^* \cdot (1 + [S]/K_m)$$